

Available online at [www.sciencedirect.com](http://www.sciencedirect.com)**SciVerse ScienceDirect**

Procedia Engineering 25 (2011) 803 – 806

**Procedia  
Engineering**[www.elsevier.com/locate/procedia](http://www.elsevier.com/locate/procedia)

Proc. Eurosensors XXV, September 4-7, 2011, Athens, Greece

## A microfluidic system for full hydrodynamic focusing control

N. Moscelli<sup>a,\*</sup>, V. Malvaioli<sup>a</sup>, F. Iuliano<sup>b</sup>, M.J. Vellekoop<sup>a</sup><sup>a</sup>*Institute of Sensor and Actuator Systems, Vienna University of Technology, Gusshausstrasse 27-29/E366, 1040, Vienna, Austria*<sup>b</sup>*Institute of Virology, Slovak Academy of Sciences, Dubravska Cesta 9, 84245, Bratislava, Slovak Republic*

### Abstract

In this contribution we present an automated microfluidic system that allows the full control of a hydrodynamically focused sample stream, both in position and width. The basis of the system is a microfluidic chip for hydrodynamic focusing. A dyed sample is optically detected by a CMOS camera mounted on a microscope. The optical setup yields a resolution of 0.5  $\mu\text{m}/\text{pixel}$ . By performing colour intensity analysis on acquired frames, the sample stream position and width are derived. With these parameters, the flowrates of programmable volume driven syringe pumps are actuated. The microfluidic system has been designed, validated, and successfully tested in time domain. Furthermore, the system design approach can be easily adapted for different microfluidic geometries.

© 2011 Published by Elsevier Ltd. Open access under [CC BY-NC-ND license](http://creativecommons.org/licenses/by-nc-nd/3.0/).*Keywords:* microfluidics; hydrodynamic focusing; optical detection; syringe pumps actuation; dye intensity analysis; Proportional-Integral control

### 1. Introduction

Precise control of hydrodynamic focusing characteristics is of importance to achieve high flow accuracy and reproducibility in the time domain. These requirements are crucial for several applications, where a hydrodynamically focused sample stream is addressed to well defined portions of the microchannel. In microfluidic cytometers, the sample stream is used as a cell/particle carrier to maximize the device sensitivity by serial analysis over an array of sensors [1]. The sample stream can also be used as a drug carrier over a culture of adherently grown cells placed on the

### Nomenclature

$Q_l$	actuation variable / volumetric flowrate of the left sheath liquid [ $\mu\text{l}/\text{min}$ ]		
$Q_r$	volumetric flowrate of the right sheath liquid [ $\mu\text{l}/\text{min}$ ]	$w(t)$	sample stream width [ $\mu\text{m}$ ]
$Q_{ss}$	volumetric flowrate of the sample liquid [ $\mu\text{l}/\text{min}$ ]	$x_d(t)$	desired sample stream position signal [ $\mu\text{m}$ ]
$Q_{sh}$	volumetric flowrate of the back sheath liquid [ $\mu\text{l}/\text{min}$ ]	$w_d(t)$	desired sample stream width signal [ $\mu\text{m}$ ]
$k$	actuation variable / flowrate gain factor	$e_x(t)$	sample stream position error [ $\mu\text{m}$ ]
$x(t)$	sample stream position [ $\mu\text{m}$ ]	$e_w(t)$	sample stream width error [ $\mu\text{m}$ ]

\* Corresponding author Tel : +43-1-58801-36625; fax: +43-1-58801-36699

E-mail address: [nicola.moscelli@tuwien.ac.at](mailto:nicola.moscelli@tuwien.ac.at)

bottom of the microchannel. In on-chip microfluidic cell patterning, wounds can be realized over a cell monolayer for collective cell migration studies [2]. Lee *et al.* have developed a theoretical model describing symmetric and asymmetric hydrodynamic focusing effect in rectangular microchannels [3]. However, the derived closed-form expressions that relate the flowrates with the sample stream dimensions are defined only in steady state, and are ideally valid for channel aspect ratios of 0 and  $\infty$ . For these reasons, a fine control over flow dynamics is required. In a previous work we presented a SISO (Single Input, Single Output) microfluidic control system for accurate sample stream positioning [4]. In this work, we have enabled full control of the hydrodynamically focused sample stream, in position and width, by realizing a DIDO (Dual Input, Dual Output) microfluidic control system.

## 2. Microfluidic control system design

As shown in Fig. 1a, the microfluidic system consists of two Proportional-Integral (PI) control units. One operates on the left sheath liquid flowrate  $Q_l$  (whose sum with the right sheath liquid flowrate  $Q_r$  is set to a constant value) to adjust sample stream position  $x(t)$ , while the other PI controller modulates the width of the sample stream  $w(t)$  by tuning a gain factor  $k$ , which multiplies the lateral flowrates (thus, increasing/decreasing both  $Q_l$  and  $Q_r$ ). The flowrates of the back sheath liquid and the sample liquid are kept constantly to 1  $\mu\text{l/min}$ . Volume driven syringe pumps (neMESYS, Cetoni GmbH, Korbussen, Germany) are employed for the flowrate actuation.

The microfluidic chip featuring hydrodynamic focusing used in our system is shown in Fig. 1b. It consists of a dual glass-silicon layer structure with 50  $\mu\text{m}$ -thick patterned SU-8 resist used to define the microfluidic channels. The hydrodynamic focusing section is realized by a  $90^\circ$  cross junction, and the optical measurements are performed at the downstream 160  $\mu\text{m}$ -wide microchannel (measurement area). The microfluidic ports (inlets and outlet), on the silicon layer, are fabricated by anisotropic silicon etching. Further detailed information on the chip fabrication process can be found in [5]. A custom made holder ensures support to the microfluidic chip and tight connection to the syringes with Teflon tubes through a PDMS gasket.

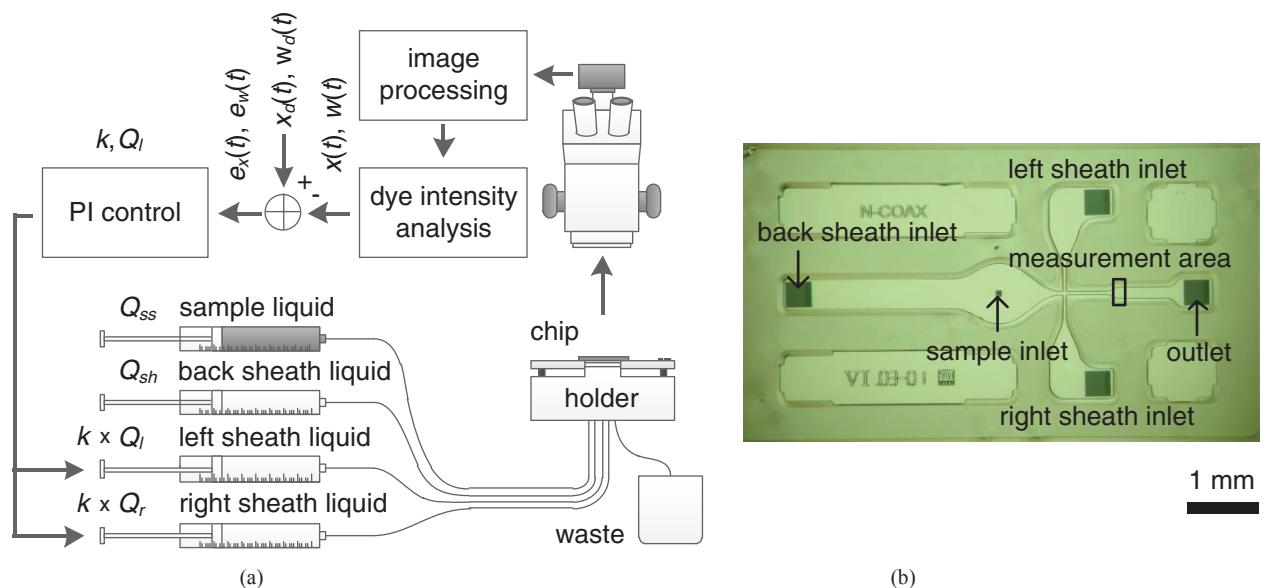


Fig. 1. (a) Block diagram of the microfluidic control system setup. The PI controllers operate on the actuation variables  $Q_l$  and  $k$ , minimizing the position and width errors,  $e_x(t)$  and  $e_w(t)$ ; (b) Photomicrograph of the hydrodynamic focusing chip (7 mm  $\times$  4 mm, patterned SU-8 resist between Si and glass layers); the liquid volume in the chip amounts to approximately 125 nl [6].

Optical detection with a resolution of 0.5  $\mu\text{m}/\text{pixel}$  is provided by a CMOS camera (Moticam 2500, Motic Group Co. Ltd.) mounted on a microscope (Stemi SV11 Apo, Carl Zeiss AG, Germany). The sample stream is optically visible as it is dyed, while de-ionized water is employed as sheath liquid. Image processing is performed on the acquired frames by subtracting them by a reference frame, previously acquired without dyed sample stream. In Fig. 2, the sample stream detection by dye intensity analysis is shown. The picture clearly shows that by the dye intensity profile shape, information on sample stream position and width can be extracted.

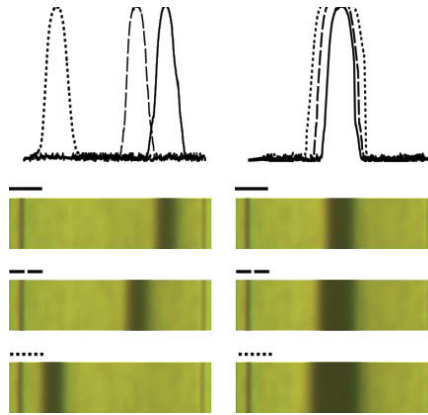


Fig. 2. Sample stream detection by dye intensity analysis. Typical intensity distributions corresponding to different sample stream widths and positions within the 160  $\mu\text{m}$ -wide measurement area.

### 3. Results and discussion

To investigate the behavior of the microfluidic system, identification experiments have been carried out to calculate an open-loop model. In these experiments, data  $Q_I$  (and thus  $Q_r$ ) was ranging from 0.5 to 19.5  $\mu\text{l}/\text{min}$ , while  $k$  was varying between 0.25 and 2.5. These settings have been chosen to span sample stream positions in close proximity of both channel walls and achieve sample widths ranging between 10% and 30% of the channel section. On the basis of a set of 8 experiments for both sample stream position and width parameters (with more than 10,000 data points acquired), a NARX model (Nonlinear Auto-Regressive model with the eXogenous input) of the system has been computed. Then, closed-loop simulations have been performed to derive the appropriate PI gains needed to achieve first order time domain behavior of position and width signals.

In order to prove the stability of sample stream properties in time domain, two simultaneous stepwise reference signals  $x_d(t)$  and  $w_d(t)$  have been used to test the feedbacks of the microfluidic control system. In Fig. 3, the simulated and measured variations of sample stream position (upper plot) and width (lower plot) are shown. A typical first order signal evolution can be observed for both sample stream position and width. The achieved sample stream position control during the experiment is in perfect agreement with the simulated system response with a settling time of 55 s. This shows a highly reproducible time domain behavior in correspondence to the position step, regardless of the sample stream position in the microchannel. The width signal shows slightly broader fluctuations, especially in the 50  $\mu\text{m}$ -width region. Nevertheless, such fluctuations are one order of magnitude lower than normal adherent cell dimensions (about 20  $\mu\text{m}$  diameter). The response of the width signal to the step reference signal obtained experimentally is somewhat faster than the simulated one, with up to 20 s shorter settling times.

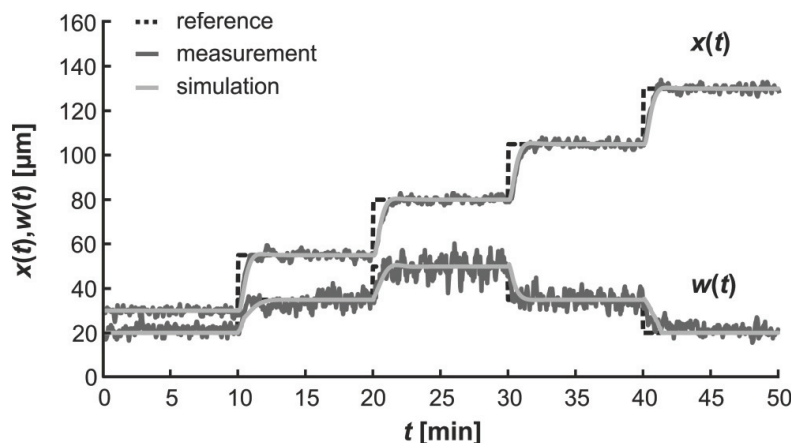


Fig. 3. Sample stream position  $x(t)$  and width  $w(t)$  in time. The reference signals  $x_d(t)$  and  $w_d(t)$  were changed stepwise simultaneously, each 10 minutes. The measured system responses are in good agreement with the simulated closed-loop responses obtained with the NARX model.

In Table 1, the obtained sample stream position and width in terms of mean value and standard deviation are shown. The mean measured sample stream positions substantially match the reference signal changes. The standard deviations are in any case below 3 pixels ( $< 1.5 \mu\text{m}$ ). The mean measured sample stream width shows a slight offset compared to the reference signal.

Table 1. Statistical data extracted from the measured sample stream position and width.

Sample stream position [ $\mu\text{m}$ ]		Sample stream width [ $\mu\text{m}$ ]	
reference $x_d(t)$	measured $x(t)$	reference $w_d(t)$	measured $w(t)$
30.0	$29.9 \pm 1.3$	20.0	$21.8 \pm 1.9$
55.0	$55.0 \pm 1.4$	35.0	$34.1 \pm 2.8$
80.0	$80.1 \pm 1.2$	50.0	$50.0 \pm 4.0$
105.0	$105.1 \pm 1.3$	35.0	$35.1 \pm 2.9$
130.0	$130.0 \pm 1.4$	20.0	$21.5 \pm 2.0$

#### 4. Conclusions

The high sample stream position and width stability obtained in the shown experiments successfully demonstrate that our microfluidic system is capable of full hydrodynamic focusing control in the time domain. This makes our control system suitable for the described applications, where high flow accuracy and reproducibility in the time domain are required. Furthermore, the identification-simulation-control approach used to design the microfluidic control system can be easily adapted to any hydrodynamic focusing chip geometry.

#### Acknowledgements

This project is part of the EU Marie Curie Research Training Network “On-Chip Cell Handling and Analysis” CellCheck (Proj. No. MRTN-CT-2006-035854, [www.cellcheck.eu](http://www.cellcheck.eu)). The project was also partly funded by the EU Erasmus Placement Program.

#### References

- [1] Kostner S, Vellekoop MJ. Interpretation of projection cytometer signals for cell analysis. *Sens Act B Chem* 2008;**132**:631–636.
- [2] van der Meer AD, Vermeul K, Poot AA, Feijen J. A microfluidic wound-healing assay for quantifying endothelial cell migration. *Am Physiol Heart Circ Physiol* 2009;**298**:H719–H725.
- [3] Lee GB, Chang CC, Huang SB, Yang RJ. The hydrodynamic focusing effect inside rectangular microchannels. *J Micromech Microeng* 2006;**16**:1024–1032.
- [4] Moscelli N, Ladisa N, Vellekoop MJ. Automated microfluidic sample stream position control for on-chip selective drug delivery. Proc. IEEE International Symposium on Computer Communication Control and Automation (IEEE 3CA) 2010, Tainan (Taiwan), Vol. 1, pp. 442–445.
- [5] Svasek P, Svasek E, Lendl B, Vellekoop MJ. Fabrication of miniaturized fluidic devices using SU-8 based lithography and low temperature wafer bonding. *Sens Act A Phys* 2004;**115**:591–599.
- [6] Hairer G, Pärre GS, Svasek P, Jachimowicz A, Vellekoop MJ. Investigations of micrometer sample stream profiles in a three-dimensional hydrodynamic focusing device. *Sens Act B Chem* 2008;**132**:518–524.